Geometrical Properties of Simulated Packings of Spherocylinders

Monika Bargieł

Institute of Computer Science, AGH University of Science and Technology
al. Mickiewicza 30, 30-059 Kraków, Poland
mbargiel@uci.agh.edu.pl

Abstract. In a wide range of industrial applications there appear systems of hard particles of different shapes and sizes, known as "packings". In this work, the force-biased algorithm, primarily designed to model close packings of equal spheres, is adapted to simulate mixtures of spherocylindrical particles of different radii and aspect ratios. The packing densities of simulated mono and polydisperse systems, are presented as functions of particle elongation and different algorithm parameters. It is shown that spherocylinders can pack more densely than spheres, reaching volume fraction as high as 0.705.

1 Introduction

Historically, dense random close packings (RCP) of spheres were considered as a model for the structure of liquids, especially those of the noble gases. RCP was viewed as a well-defined state [1] with density $\phi \approx 0.6366$. This value was obtained in experiments [2] [3] as well as computer simulations [4]. Later work by Jodrey and Tory [5] and Mościński et al. [6] showed that higher densities could be easily obtained at the cost od increasing the order in the sphere system. Since the precise definition of "randomness" is lacking, the distinction between ordered and random is not absolute. Bargieł and Tory [7] introduced the measure of local disorder as the deviation of each 13-sphere complex from the corresponding fragment of either f.c.c. or h.c.p. lattice. The global disorder is then defined as the average local disorder (see formulae (21) to (23) of [7]). This measure enables to identify crystalline or nearly crystalline regions and hence to track the transition from RCP to the higher densities and determine the extent to which the greater density increases the order. Approximating the fraction of quasi-crystalline fragments (f.c.c. or h.c.p.) versus packing density they observed that the first crystalline fragments begin to form in the random structure at $\phi \approx 0.6366$ (see Fig. 7 and Table 6 of [7]), the value close to the earlier predictions for RCP.

Recently, Torquato et al. [8] described RCP is an ill-defined state and introduced the concept of the maximally random jammed (MRJ) state [9] [10], corresponding to the least ordered among all jammed packings. For a variety of order metrics, it appears that the MRJ state has a density of $\phi \approx 0.6366$ and again is consistent with what has been thought of as RCP [11].

M. Bubak et al. (Eds.): ICCS 2008, Part II, LNCS 5102, pp. 126–135, 2008.

There exist a wide spectrum of experimental and computational algorithms that can produce packings of equal spheres of different porosity and geometrical properties [12] [13] [6] [14] [15] [4] [5] [16]. However, in many applications we have to deal with granular systems of hard particles which are far from spherical. Those non-spherical particles have to be treated in quite different way due to their additional rotational degrees of freedom.

Recently, Donev et al. [17] [18] and independently Bezrukov et al. [19] adapted some of the known algorithms to produce random packings of ellipsoids. Donev et al. [20] experimented with two kinds of M&M's®Candies, and then they generalized the well known Lubaschevsky-Stillinger algorithm (LS) [12] [13] to handle ellipsoids. In both cases (experiment and simulation) they obtained high volume fractions (up to 0.71). Abreu et al. [21] used the Monte Carlo technique to study the packings of spherocylinders in the presence of gravitational field.

In this paper we used the adaptation of the force-biased (FB) algorithm [6] [14] to produce dense random packings of spherocylinders. The reason for this choice is that spherocylinders are excellent model for particles from spherical to very elongated (rod-like) depending on their aspect ratio. Furthermore there exists an efficient algorithm to calculate the distance between two spherocylinders and to detect potential overlaps [22] [21], which is crucial in practically any dense packing simulation process. Furthermore, Allen et al. [23] argue, that spherocylinders show a smectic phase (while ellipsoids do not), since they can be mapped onto the hard sphere fluid by the global change of scale.

We tested two systems of hard spherocylinders: isotropic and nematic. In the isotropic system the spherocylinders have random initial orientation, which is constant throughout the simulation. To observe the isotropic - nematic transition we allowed for the rotation of the spherocylinders with different ratios. In this case we obtained much higher densities at the cost of increasing the value of the nematic order parameter [23].

2 The Force-Biased Algorithm

2.1 Spheres

The force-biased (FB) algorithm was primarily designed to attain very dense irregular packings of hard spheres [6] [14]. The initial configuration of the system is a set of N (initially overlapping) spheres centered at $\boldsymbol{r}_i$, $i = 1, \ldots, N$ and of diameter d_i chosen according to a given distribution function. The algorithm attempts to eliminate overlaps by pushing apart overlapping particles while gradually reducing their diameters as described in [6] [14]. The spheres are moved according to the repulsive "force", $\boldsymbol{F}_{ij}$, defined between any two overlapping particles. The new position of the i-th sphere is then given by

$$\boldsymbol{r}_i = \boldsymbol{r}_i + \varepsilon \sum_{j \neq i} \boldsymbol{F}_{ij} \,, \tag{1}$$

and

$$\boldsymbol{F}_{ij} = \alpha_{ij} p_{ij} \frac{\boldsymbol{\delta}_{ij}}{|\boldsymbol{\delta}_{ij}|} \,, \tag{2}$$

where ε is the scaling factor, and α_{ij} is the overlap index

$$\alpha_{ij} = \begin{cases} 1 & \text{if particles } i \text{ and } j \text{ intersect} \\ 0 & \text{otherwise.} \end{cases} \tag{3}$$

The pair "potential", p_{ij}, is proportional to the overlap between spheres i and j. For monosized spheres (of diameter d) the definition of p_{ij}, is straightforward

$$p_{ij} = d\,(1 - \frac{\delta_{ij}^2}{d^2})\,, \tag{4}$$

where δ_{ij} is the distance between the centers of the spheres i and j, i.e.

$$\delta_{ij}^2 = |\boldsymbol{r}_{ij}|^2\,. \tag{5}$$

However, (4) cannot be applied efficiently to spheres of different diameters (especially when the difference in sizes is large). Hence, for diameters of arbitrary distribution, another potential function was devised (similar to those given in [19])

$$p_{ij} = d_1 \frac{d_j}{d_i} \left[1 - \frac{\delta_{ij}^2}{\frac{1}{4}(d_i + d_j)^2} \right]\,. \tag{6}$$

For equal particles $d_i = d$, $i = 1, \ldots, N$ and (6) simplifies to (4).

2.2 Adaptation to Spherocylinders

Using spherocylinders instead of spheres complicates the algorithm for couple of reasons. Firstly, a spherocylinder, i, is described by four parameters. In addition to its diameter, d_i, and spatial position, $\boldsymbol{r}_i$, we have to consider the length of its cylindrical portion, l_i, and orientation of its main axis, given by a unit vector $\boldsymbol{u}_i$. What is more important, the overlap detection and calculating the potential function between two spherocylinders is much more complicated than for the case of spheres. Vega and Lago [22] proposed a very efficient algorithm for locating the minimum distance between spherocylinders, later improved by Abreu et al. [21]. This algorithm uses the notion of a shaft of a spherocylinder as the main axis of its cylindrical portion. The coordinates of any point of a shaft i are given by

$$\boldsymbol{s}_i = \boldsymbol{r}_i + \lambda_i \boldsymbol{u}_i\,, \tag{7}$$

where $\lambda_i \in [-l_i/2, l_i/2]$. Spherocylinders i and j overlap if the shortest distance between their shafts, δ_{ij}, is less then the sum of their radii, that is, when $\delta_{ij} < (d_i + d_j)/2$. Let $\boldsymbol{q}_i = \boldsymbol{r}_i + \lambda_i^{*(j)} \boldsymbol{u}_i$ and $\boldsymbol{q}_j = \boldsymbol{r}_j + \lambda_j^{*(i)} \boldsymbol{u}_j$ are the points on shafts i and j, respectively, closest to each other. Then

$$\boldsymbol{\delta}_{ij} = \boldsymbol{q}_j - \boldsymbol{q}_i = \boldsymbol{r}_{ij} + \lambda_j^{*(i)} \boldsymbol{u}_j - \lambda_i^{*(j)} \boldsymbol{u}_i \tag{8}$$

is the vector connecting the closest points of shafts i and j, and

$$\delta_{ij}^2 = |\boldsymbol{\delta}_{ij}|^2\,. \tag{9}$$

For parallel shafts (e.i. when $|\boldsymbol{u}_i \cdot \boldsymbol{u}_j|^2 = 1$) their distance can be expressed as

$$\delta_{ij}^2 = |\boldsymbol{r}_{ij}|^2 - |\boldsymbol{u}_i \cdot \boldsymbol{r}_{ij}|^2 + \left[\max(0, |\boldsymbol{u}_i \cdot \boldsymbol{r}_{ij}| - \frac{l_i + l_j}{2})\right]^2 . \tag{10}$$

Equation (10) can be applied for calculating overlaps between a sphere and a spherocylinder. A sphere i can be considered as a spherocylinder of null length ($l_i = 0$) and parallel to particle j ($\boldsymbol{u}_i = \boldsymbol{u}_j$ or $\boldsymbol{u}_i = -\boldsymbol{u}_j$). Obviously when $l_i = l_j = 0$ (both particles are spheres) we get (5).

In addition to shifting the positions of the particles (see (1)), the spherocylinders can be rotated according to

$$\boldsymbol{u}_i = n\left(\boldsymbol{u}_i - \varepsilon_r \frac{d_i}{l_i} \sum_{i \neq j} \alpha_{ij} p_{ij}^r \lambda_i^{*(j)} \frac{\boldsymbol{\delta}_{ij}^r}{|\boldsymbol{\delta}_{ij}^r|}\right) , \tag{11}$$

where p_{ij}^r is the rotational potential

$$p_{ij}^r = 1 - \frac{\delta_{ij}^2}{\frac{1}{4}(d_i + d_j)^2} , \tag{12}$$

$\boldsymbol{\delta}_{ij}^r$ is the projection of $\boldsymbol{\delta}_{ij}$ onto the plane perpendicular to $\boldsymbol{u}_i$, given by

$$\boldsymbol{\delta}_{ij}^r = \boldsymbol{\delta}_{ij} - \boldsymbol{u}_i(\boldsymbol{\delta}_{ij} \cdot \boldsymbol{u}_i) , \tag{13}$$

ε_r is the scaling factor, and $n(\boldsymbol{x}) = \boldsymbol{x}/|\boldsymbol{x}|$ is the unit vector in the direction of $\boldsymbol{x}$.

In the case of spheres, when all the overlaps are eliminated, the algorithm stops. For spherocylinders the density can be further increased when, after elimination of overlaps, the size of the particles is increased by a certain factor and the overlap elimination process is repeated. This is done until further densification is not possible.

3 Results

We present results obtained from the FB algorithm for monodisperse systems and binary mixtures of spherocylinders. The objective of this study was to verify the influence of the particle size distribution, shape (e.i. the aspect ratio), and rotation factor, ε_r, on the packing density and the orientational order of the system represented by the nematic order parameter, S.

3.1 Monodisperse Systems

In this section the packing fraction of the monodisperse beds of spherocylinders is studied using the FB algorithm. Each simulation was performed in a cubic container with periodic boundary conditions. We used systems of N particles of aspect ratios, γ, ranging from 0 (spheres) to 80 (very long rods). The value

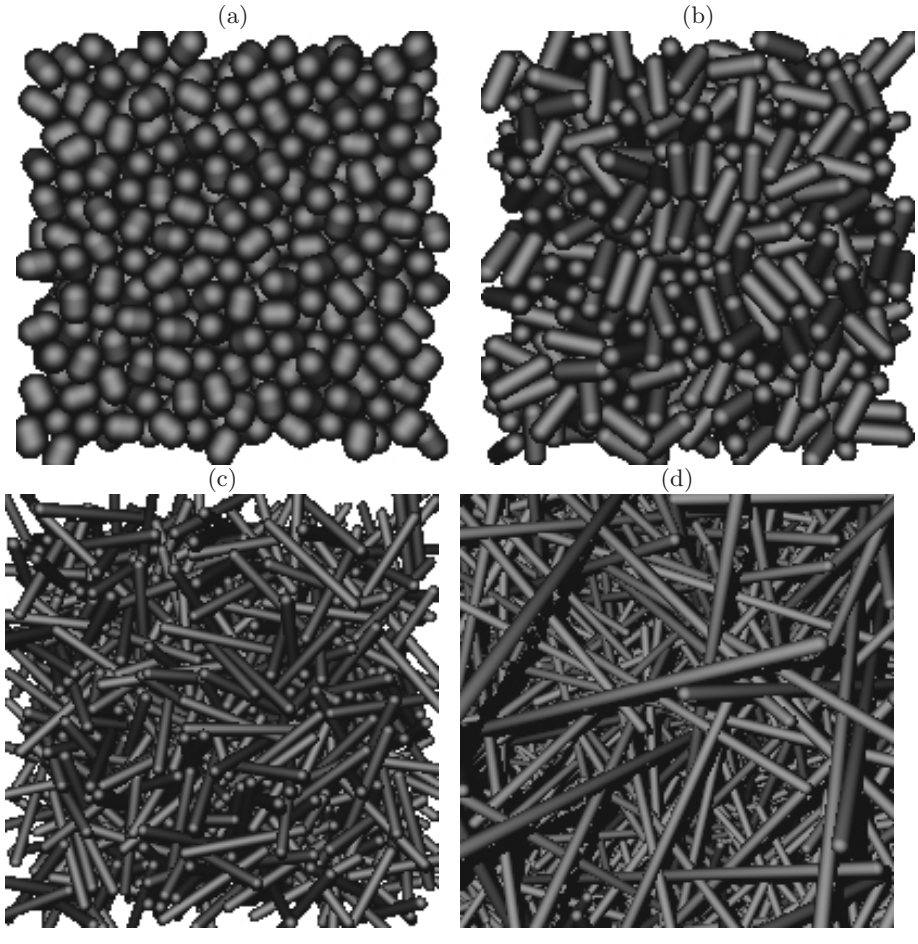

Fig. 1. Sample packings of spherocylinders (a) $\gamma = 0.4$, (b) $\gamma = 2$, (c) $\gamma = 10$, (d) $\gamma = 80$

of N was 2000 for $\gamma \leq 20$ but it had to be increased to 6000 for $\gamma = 40$ and to 15000 for $\gamma = 80$ due to the periodic boundary condition requirements, that size of any particle cannot exceed half of the computational box length, L. For monodisperse packings the number of spheres required, N, can be estimated on the basis of the nominal packing density, η_0, which never can be exceeded by the actual volume fraction. For details on the meaning of the nominal and actual packing densities see [6] [14]. Additionally, if d_0 is the diameter of the spherocylinder corresponding to η_0, its volume, v_0, is given by

$$v_0 = \frac{\pi d_0^3}{6}(1.5\gamma + 1)\,. \tag{14}$$

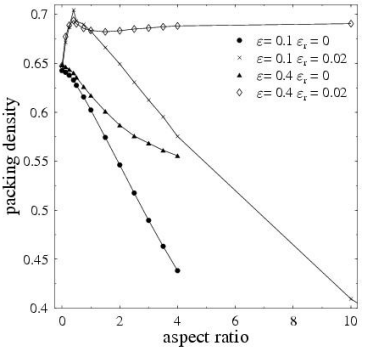

Fig. 2. Dependence of the packing density on the aspect ratio for different values of ε and ε_r

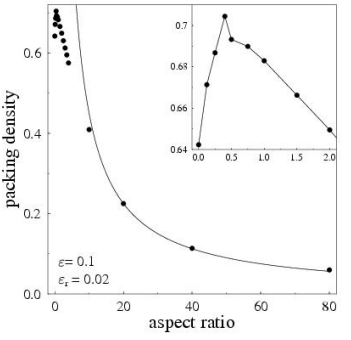

Fig. 3. Dependence of the packing density on the aspect ratio for $\varepsilon = 0.1$ and $\varepsilon_r = 0.02$. The inset is a blowup of the upper left corner of the main figure.

Consequently, the packing density, η_0, is

$$\eta_0 = N v_0 / L^3 \,. \tag{15}$$

From the periodic boundary condition

$$d_0(\gamma + 1) < \frac{1}{2} L \,, \tag{16}$$

it is easy to obtain

$$N > \frac{48(\gamma + 1)^3}{\pi(1.5\gamma + 1)} \, \eta_0 \,. \tag{17}$$

We start from the isotropic configuration in which particle centers are uniformly distributed in the box and orientations are taken uniformly from the unit sphere. By setting $\varepsilon_r = 0$ we disable rotations and ensure that the final orientations are globally isotropic. It is possible, however, that some positional order will appear in the final configuration. When $\varepsilon_r > 0$ rotations are allowed and some orientational order can appear as well. We measure the degree of orientational order calculating the well known nematic order parameter, S, [23].

The results obtained for spherocylinders depended strongly on the aspect ratio, γ. Images (formed by the Persistence of Vision Raytracer, povray, version 3.6.1 [24]) of the random packings for several aspect ratios may be seen in Fig. 1. In all cases rotations were allowed ($\varepsilon_r = 0.02$).

Fig. 2 shows the dependence of the final packing density on the aspect ratio for different values of the rotation factor, ε_r, while Fig. 3 presents the same dependance for $\varepsilon = 0.1$, $\varepsilon_r = 0.02$ and it covers much wider range of aspect ratios. Each point is an average over 10 runs. It is apparent from the figures that the packing density increases with γ up to a certain value. Further increase of γ

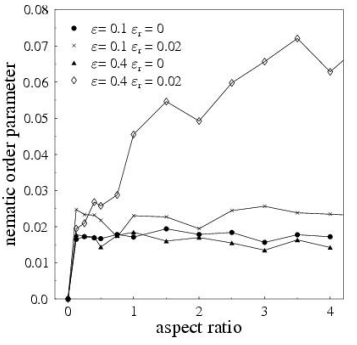

Fig. 4. Dependence of the nematic order parameter, S, on the aspect ratio

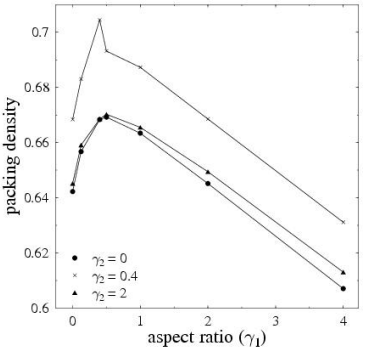

Fig. 5. Dependence of the packing density of the bidisperse mixture on the aspect ratios, γ_1 and γ_2, for $\varepsilon = 0.1$ and $\varepsilon_r = 0.02$

causes a density decrease. That means that there exists an aspect ratio, γ_m, for which spherocylinders can be packed the densest. This value does not depend on the rotation factor, although obviously the densities obtained for various ε_r are different. The experimental points in Fig. 3 lie on the line $\phi = 4.5/\gamma$ (solid line in the figure) for $\gamma > 10$, which is in very good agreement with theory [21].

Fig. 4 shows the development of the orientational order in the system, represented by the nematic order parameter, S, vs. γ, and ε_r. As could be expected the nematic order parameter is very small (below 0.02) for $\varepsilon_r = 0$, since in this case no rotations are allowed and the directional order remains random. For $\varepsilon_r = 0.02$ and $\varepsilon = 0.1$ values of S are only slightly higher but for $\varepsilon_r = 0.02$ and $\varepsilon = 0.4$, S reaches almost 0.08. This is the effect of much faster movement which enables spherocylinders of similar orientation to group. This can be observed in the figures not shown in this paper.

3.2 Bidisperse Mixtures

Aiming at verifying the effect of particle shape on the packing density and ordering of binary mixtures of spherocylinders, FB simulations were carried out using two species of particles with different aspect ratios. Each species is composed of certain number of particles (N_1 and N_2 respectively) with a specific aspect ratio (γ_1 and γ_2). In order to focus on shape effects, all the simulated particles have the same volume.

Fig. 5 shows the dependence of the total packing density of the binary mixture on the aspect ratios, γ_1, and γ_2. It can be observed that the highest density is attained for $\gamma_1 = \gamma_2 = 0.4$ (monodisperse case). The shape of the function $\phi(\gamma_1)$ is similar for all values of γ_2 used, but for $\gamma_2 = 0.4$ the density is much higher than for other values. Also only for $\gamma_2 = 0.4$ there is a characteristic peak of density.

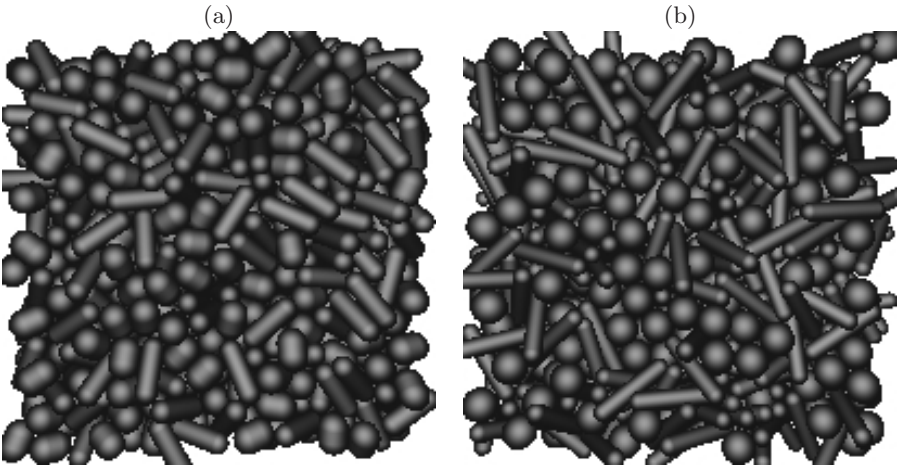

Fig. 6. Sample packings of bidisperse mixtures for $\varepsilon = 0.1$ and $\varepsilon_r = 0.02$ (a) $\gamma_1 = 0.4$, $\gamma_2 = 2$ (b) $\gamma_1 = 0$, $\gamma_2 = 4$

Fig. 6(a) shows sample packing of a binary mixture with $\gamma_1 = 0.4$ and $\gamma_2 = 2$, while in Fig. 6(b) $\gamma_1 = 0$ (spheres) and $\gamma_2 = 4$.

4 Conclusions

The force-biased algorithm for obtaining granular packings has been adapted to handle spherocylinders out to very large aspect ratios. The results for the spherocylinders reproduce existing experimental results for all available aspect ratios [21]. The volume fractions of the long spherocylinders confirm the prediction that the random packing density of thin rods is inversely proportional to the aspect ratio. The agreement is excellent for γ above 10. Our simulation results also agree fairly well with the available experimental densities. For a comparison of simulation and experimental packing densities see Fig. 6 of [25]. Most experiments presented relate to granular rods or fibers from a variety of materials such as wood, metal wire, and raw spaghetti. It is believed that the scatter of experimental densities are due to factors such as wall effects, friction, local nematic ordering, and particle flexibility [25].

The random sphere packing density turns out to be a local minimum: the highest density occurs at an aspect ratio of $\gamma \approx 0.4$. The practical implication is that a small deviation in shape from spherical may increase the random packing density significantly without crystallization. It is clear that a polydisperse system of spheres packs more densely than a monodisperse system. For equally sized closely packed spheres the interstices between the particles are small enough such that no additional spheres can be placed in them. If the system is made more and more polydisperse, the smaller spheres may be placed where the larger ones previously could not. Perturbing the particle shape from spherical has a

similar effect: a short spherocylinder that may not fit when oriented in a given direction may fit when the orientation is changed.

Finally, our simulations clearly show that particles with a given aspect ratio have a unique random packing density: The Bernal sphere packing can be generalized to spherocylinders of arbitrary aspect ratio with one and the same simulation method. This indicates that these packings all follow the same geometrical principle.

The parameters of the FB algorithm strongly influence the final packing density of a given mixture as well as the orientational ordering of the resulting bed. Careful choice of these parameters is crucial for the efficiency of the algorithm and properties of the resulting packings. As long as $\varepsilon_r = 0$ the bed remains isotropic. When $\varepsilon_r > 0$ but ε is small (particles are not allowed to move too quickly) the bed is only slightly more ordered. However, when we increase ε, the orientational order quickly raises producing packings in the nematic phase.

It should be possible to study other shapes of particle such as ellipsoids and disks using this method. The only issue here is to find an effective algorithm to calculate the distances between particles of a given shape. Otherwise the adaptation is straightforward. Since there are many computer and experimental studies concerning packings of ellipsoids [17] [18] [20], this is the more probable next step in this research. Also the packing of disks presents an interesting problem. Nevertheless the geometry of a disk, though simple, shows nontrivial difficulties in the calculations.

Acknowledgement. Partial support of the AGH Grant No. 11.11.120.777 is gratefully acknowledged.

References

1. Bernal, J.D.: A geometrical approach to the structure of liquids. Nature 183, 141–147 (1959)
2. Scott, G.D., Kilgour, D.M.: The density of random close packing of spheres. Brit. J. Appl. Phys. 2, 863–866 (1964)
3. Finney, J.L.: Random packing and the structure of simple liquids. Proc. Roy. Soc. A 319, 470–493 (1970)
4. Jodrey, W.S., Tory, E.M.: Computer simulation of isotropic, homogeneous, dense random packing of equal spheres. Powder Technol. 30, 111–118 (1981)
5. Jodrey, W.S., Tory, E.M.: Computer simulation of close random packing of equal spheres. Phys. Rev. A 32, 2347–2351 (1985)
6. Mościński, J., Bargieł, M., Rycerz, Z.A., Jacobs, P.W.M.: The force-biased algorithm for the irregular close packing of equal hard spheres. Molecular Simulation 3, 201–212 (1989)
7. Bargieł, M., Tory, E.M.: Packing fraction and measures of disorder of ultradense irregular packings of equal spheres. II. Transition from dense random packing. Advanced Powder Technology 12(4), 533–557 (2001)
8. Torquato, S., Truskett, T.M., Debenedetti, P.G.: Is random close packing of spheres well defined? Phys. rev. Letters 84(10), 2064–2067 (2000)

9. Donev, A., Torquato, S., Stillinger, F.H., Conelly, R.: Jamming in hard sphere and disk packings. J. Appl. Phys. 95(3), 989–999 (2004)
10. Donev, A., Torquato, S., Stillinger, F.H., Conelly, R.: A liner programming algorithm to test for jamming in hard sphere packings. J. Comp. Phys. 197(1), 139–166 (2004)
11. Kansal, A.R., Torquato, S., Stillinger, F.H.: Diversity of order ans densities in jammed hard-particle packings. Phys. Rev. E 66, 41109 (2002)
12. Lubachevsky, B.D., Stillinger, F.H.: Geometric properties of random disk packing. J. Stat. Phys. 60, 561–583 (1990)
13. Lubachevsky, B.D., Stillinger, F.H., Pinson, E.N.: Disks vs. spheres: Contrasting properties of random packings. J. Stat. Phys. 64, 501–525 (1991)
14. Mościński, J., Bargieł, M.: C-language program for simulation of irregular close packing of hard spheres. Computer Physics Communication 64, 183–192 (1991)
15. Bargieł, M., Tory, E.M.: Packing fraction and measures of disorder of ultradense irregular packings of equal spheres. I. Nearly ordered packing Advanced Powder Technol. 4, 79–101 (1993)
16. Zinchenko, A.Z.: Algorithm for random close packing of spheres with periodic boundary conditions. J. Comp. Phys. 114(2), 298–307 (1994)
17. Donev, A., Torquato, S., Stillinger, F.H.: Neighbor list collision-driven molecular dynamics simulation for nonspherical particles. I. Algorithmic details. Journal of Computational Physics 202, 737–764 (2005)
18. Donev, A., Torquato, S., Stillinger, F.H.: Neighbor list collision-driven molecular dynamics simulation for nonspherical particles. II. Applications to ellipses and ellipsoids. Journal of Computational Physics 202, 765–773 (2005)
19. Bezrukov, A., Bargieł, M., Stoyan, D.: Statistical analysis of Simulated Random Packings of Spheres. Part. Part. Syst. Charact. 19, 111–118 (2002)
20. Donev, A., Cisse, I., Sachs, D., Variano, E.A., Stillinger, F.H., Connel, R., Torquato, S., Chaikin, P.M.: Improving the density of jammed disordered packing using ellipsoids. Science 303, 990–993 (2004)
21. Abreu, C.R.A., Tavares, F.W., Castier, M.: Influence of particle shape on the packing and on the segregation of spherecylinders via Monte Carlo simulations. Powder Technology 134, 167–180 (2003)
22. Vega, C., Lago, S.: A fast algorithm to evaluate the shortest distance between rods. Computers and Chemistry 18(1), 55–59 (1994)
23. Allen, M.P., Evans, G.T., Frenkel, D., Muldner, B.M.: Hard Convex Body Fluids. Advances in Chemical Physics 86, 1–166 (1993)
24. `http://www.povray.org`
25. Williams, S.R., Philipse, A.P.: Random Packings of spheres and spherocylinders simulated by mechanical contraction. Phys. Rev. E 67, 51301 (2003)